Turkish Journal of Physics

http://journals.tubitak.gov.tr/physics/

Research Article

Turk J Phys
(2018) 42: 587 – 599

doi:10.3906/fiz-1803-6

On differential depletion length of Schottky diodes with copper-nickel alloy metal of front contact

Abdulkadir KORKUT*
Department of Physics, Faculty of Sciences, Van Yüzüncü Yıl University, Van, Turkey

Received: 06.03.2018 • **Accepted/Published Online:** 03.09.2018 • **Final Version:** 12.10.2018

Abstract: This work was prepared in two sections; the first section describes how to alloy Schottky diodes and aims to understand how metal alloys affect the essential parameters of Schottky diodes at the metal–semiconductor interface. The second section covers the varying differential depletion length in (Cu% Ni%)/n–Si/Al binary-alloyed Schottky diodes. After collecting data, the characteristics of Schottky diodes are calculated by plotting them with an increasing percentage ratio of the first element. We see that alloyed Schottky diode characteristics significantly depend on the mass percentage ratio of the first element. Significant results are seen: first, V_{bi} (built-in potential) directly affects the characteristics of Schottky diodes with a turning point occurring at the V_{bi} point on the axis, and second, the built-in potential plays a key role in Schottky diode characteristics. Estimation of the depletion length depends on the built-in potential. For the forward and reverse bias cases, the depletion length versus voltage graphs are identical, but with their symmetry mirrored. Analyzing the differential depletion lengths, it is easily seen that they have higher or lower values compared to the zero depletion length for the forward and reverse bias cases, respectively. When the depletion length formula is expanded in a series, new equations are obtained to show significant effects on Schottky diode characteristics.

Key words: Schottky alloyed metal, depletion length, differential depletion length, metal–semiconductor interface

1. Introduction

It is well known that the metal–semiconductor interface has a very significant effect on the electrical characteristics of diodes. The interface is obtained by depositing metal onto the semiconductor using the evaporation method. The difference in metal and semiconductor work functions gives the Schottky barrier height (SBH), which is one of the important parameters defining the characteristics of a Schottky diode.

If we alter the mass percentage ratio of the alloy metal in the compound used to obtain the interface, all the Schottky diode parameters will change: the ideality factor (n_{IV}) [1], barrier height (Φ_{BH}) [1], Cheung functions (Ch1, Ch2) [2], built-in potential (V_{bi}) [3], donor density (N_D) [4–6], zero bias depletion length (W_0 or L_0) [1], interfacial thickness (D_{it}) [1], interface state density (N_{SS}) [7,8] and effective Fermi level (E_F) [1,3]. In other words, the work function of the alloy metal heavily depends on the metal used and the percentage used. Therefore, SBH will vary with the amount of use and the type of metal in the compound used to produce the metal alloy [3]. There are many alloy examples in industry: cupronickel consists of Cu 70% Ni 30% (ASTM 122 as standard); Monel consists of Cu 33% Ni 67% [https://en.wikipedia.org/wiki/List_of_alloys].

We want to fabricate metal–semiconductor (MS) devices. However, organic contamination and a native oxide layer covers the semiconductor surface during the fabrication process in the laboratory environment [1,3].

*Correspondence: akkut@yyu.edu.tr

Thus, the MS devices transform into metal–insulator–semiconductor (MIS) devices due to the existence of such an insulating layer. This transformation is a reason for the strong effect on the electrical parameters of a diode [1–6]. We have to make sure that this is not the case here.

Schottky diodes are formed from four sections: 1) an ohmic junction, 2) a base structure, 3) a depletion layer, and 4) a Schottky junction [5,6]. This article is aimed at understanding the major characteristics of Schottky MS diodes, the effects of the depletion length (DL), and the differential depletion length (DDL) approximation [9] of Cu XX% Ni YY% alloy/n–Si/Al Schottky diodes with an increasing amount of the first element in terms of an alloy mass percent (m_p %) [10].

In this paper, we use a new approximation to characterize Schottky diodes. In this approximation, we use DL as a main parameter to obtain one of the main characterizations of the diode. The novelty of the present work is DL and DDL, as it is seen from the literature that DL and DDL have been expressed as formulas and sentences, but they have not been plotted as a figure for both forward and reverse bias cases [3–6]. The second novelty is an expanded series line of the DDL. Its lines give us characteristics in the case of forward and reverse bias. The angle between two lines is a specific number, and lines obey $m_1 - m_2 \approx 0$ or $m_1 \approx m_2$ (m_2: slope in the case of forward bias, m_1: slope in the case of reverse bias). The angle between two lines will be zero for an ideal state in the case of forward bias and reverse bias, i.e. both lines behave as parallel lines like the single line. Therefore, it might represent a characteristic view for Schottky diodes.

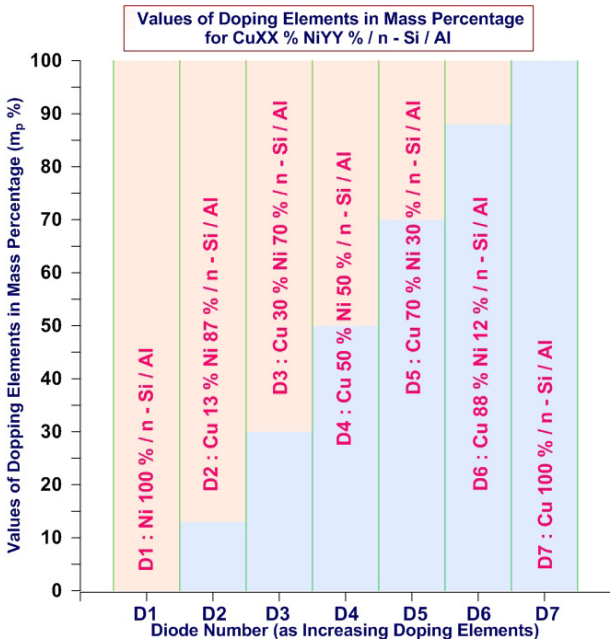

Figure 1. The values of the doping elements by percentage for Cu XX% Ni YY%/n–Si/Al Schottky diodes (Cu ratio increases from left to right).

The present work adds the depletion approximation concept to the literature, which involves depletion length, differential depletion length, depletion capacitance, differential depletion capacitance, depletion charge, and differential depletion charge for forward and reverse bias. The depletion parameters of a diode are indispensable; otherwise, it is not a diode and current is conducted one way. The reason for choosing a CuNi alloy is having a binary alloy. The mass mixing rate determines alloying ratios. Alloy ratios were chosen as

(0% Cu) (100% Ni), (10% Cu) (90% Ni), (30% Cu) (70% Ni), (50% Cu) (50% Ni), (70% Cu) (30% Ni), (90% Cu) (10% Ni), and (100% Cu) (0% Ni). The percent rate was selected as symmetric in order for the alloy ratio effect of MS Schottky diodes to be understandable.

2. Experimental details

2.1. Experimental method

In the fabrication progress of the diode, an n-Si wafer with (100) orientation was used. It has a thickness of 450 μm and a resistivity of ρ = 1 to 10 Ω cm. The wafer (n-Si) was chemically cleaned of chemical and organic contaminants. To clean wafers of contamination, the wafer was boiled in RCA (NH_4H + H_2O_2+ $6H_2O$) for 3 min, and then it was placed in (HCl + H_2O_2+ $6H_2O$) and boiled for another 3 min. Later, wafers were etched in HF:H_2O (1:10) for 30 s and rinsed in deionized water using ultrasonic vibration [9]. Then the n-Si wafer was cut into at least ten single pieces (as the surface area had to be 25 mm^2). After the cleaning and cutting process, an ohmic contact was formed in the rear of these pieces by evaporating clean Al at a pressure of 10^{-6} Torr and heating at 425 °C for 3 min with a flow of N_2 gas. The ohmic contact was formed in this way for all samples. One of the samples was immediately inserted into the evaporation chamber to avoid native oxidation. After placing the sample inside the chamber, Cu (of 5 N pure) was evaporated onto the front side of the Schottky contact under 10^{-6} Torr pressure. The same process was repeated for Ni metal (of 5 N pure). Thus, we fabricated Cu 100%/n–Si/Al, Ni 100%/n–Si/Al Schottky diodes. They were used as reference diodes because they only contained 100% Ni (labeled D1) or 100% Cu (labeled D7) elements (Figure 1; Table 1).

Table 1. The ideality factor and barrier height values of alloy metal/n–Si/Al Schottky diodes (from I–V, C–V, Ch1, Ch2 data).

Diode code	Elemental ratio in alloy	Ideality factor		Barrier height (eV)		
	(%)	n_{iv}	n_{iv-Ch1}	Φ_{BH-IV}	Φ_{BH-CsV}	$\Phi_{BH-IV-Ch2}$
D1	Ni 100%	1.053	1.072	0.634	0.936	0.529
D2	Cu 13% Ni 87%	1.025	1.085	0.621	0.922	0.527
D3	Cu 30% Ni 70%	1.039	1.052	0.666	0.921	0.621
D4	Cu 50% Ni 50%	1.037	1.048	0.678	1.170	0.762
D5	Cu 70% Ni 30%	1.022	1.037	0.714	1.202	0.863
D6	Cu 88% Ni 12%	1.065	1.095	0.594	0.851	0.497
D7	Cu 100%	1.025	1.054	0.608	0.917	0.533

2.2. Process for making the alloy

We fabricated CuNi alloys using an Edwards A310/500 evaporation chamber unit under 5 × 10^{-5} Torr vacuum. After the reference diodes had been produced, the ratio of the mass percentage of the first element was increased in the compound. Therefore, we made several samples with different amounts of the first element in the compound in terms of mass percentage. These diodes were labeled Cu XX% Ni YY%/n–Si/Al (Figure 1; Table 1).

The first stage, with a purity ratio of (5n: 99.995%), Cu (13% by mass) powder and Ni (87% by mass) powder were put into a tungsten boat and the boat was placed in the evaporation chamber. The machine

was activated to apply a current slowly stepping up to 0.01 mA by 0.01 mA. When the Cu and Ni powder transformed into liquid (by melting), the applied current was set. After this point, the applied current was slowly stepped down from 0.01 mA by 0.01 mA steps, and a Cu 13% Ni 87% alloy was obtained. After 10 s, the Cu 13% Ni 87% alloy was evaporated onto the /n–Si/Al semiconductor base at full power. All samples were made using this method. The first alloy diode, using Cu 13% Ni 87%/n–Si/Al percentages, was called D2. In addition, we followed the sequence numbering to label the rest of the samples as D3, D4, D5, and D6 for Cu 30% Ni 70%/n–Si/Al, Cu 50% Ni 50%/n–Si/Al, Cu 70% Ni 30%/n–Si/Al, and Cu 88% Ni 12%/n–Si/Al, respectively. Our alloy types were similar to ones used in industry (such as D3 and D5 diodes) (Table 1).

The ideality factor (n_{IV}, n_{Ch1}), barrier height (Φ_{IV}, Φ_{CV}, Φ_{Ch2}), built-in potential (V_{bi}), donor concentration (N_D), Fermi level (E_F), interface thickness (D_{it}), and interface state density (N_{ss}) [11] were calculated from the current–voltage (I–V) and capacitance–voltage (C_s–V) graphs [9]. The characteristics of the Schottky diodes, which depended on the voltage and the increasing mass percentage of the first element, were calculated from ln (I)–V measurements and then plotted. C_s–V measurements were done at room temperature (300 K) at a frequency of 250 kHz. After obtaining the characteristics of the Schottky diodes, we plotted three graphs for depletion length: zero bias depletion length versus increasing mass percentage of the first element ($L_0 - m_p$ %), depletion length versus positive application voltage (FB: forward bias; $L_{FB} - V_a$), and depletion length versus negative application voltage (RB: reverse bias; $L_{RB} - -V_a$) [9].

2.3. Ideality factor

The ideality factor is used to determine the main features of a diode. According to thermionic emission theory, the Schottky diode's current–voltage characteristics are already expressed in the literature [10–14]. One can find the I–V graph for different metal types in [10–14]. In the case of forward bias current for nonideal conditions, the equation is expressed as follows:

$$\boldsymbol{I = \underbrace{AR_n^* T^2 exp\left(-\frac{e\Phi_{BH}}{kT}\right)}_{I_0}\left[exp\left(\frac{e(V - IR_s)}{nkT}\right) - 1\right]}, \tag{1}$$

where n is the ideality factor, V is the forward bias voltage, e is the electron charge, R_s is the series resistance, k is the Boltzmann constant, T is the temperature in Kelvin, and I_0 is the saturation current. Additionally, R^*_n is the Richardson constant (110 A/cm^2 K^2 for n-type Si) [2,10], A is the active diode area (using a mask radius of 0.4 mm in the experiment), and Φ_{BH} is the effective barrier height.

The ideality factor (IF), n, is determined from the slope of the linear region of the forward bias in the ln (I)–V characteristic using the following relationship [2,8,10,11]. As seen from Figures 2a and 2b, fits are taken from ln (I)–V. The slope of the fits is written as in Eq. (2) and n, the ideality factor, is obtained:

$$\boldsymbol{n = \frac{e}{kT}\frac{dV}{d(lnI)}}. \tag{2}$$

The ideality factor, obtained from I–V data and Ch1, is shown in Figure 3. When Figure 3 is examined, the red line represents data obtained from the I–V graph and the green line represents data obtained from Ch1. As expected, the lines have the same characteristics. We emphasize that the alloy ratio increased towards the right-hand side and starts from 10% to 30%, 50%, 70%, 90%, and 100%. We did not include 0% because that represents the reference diodes.

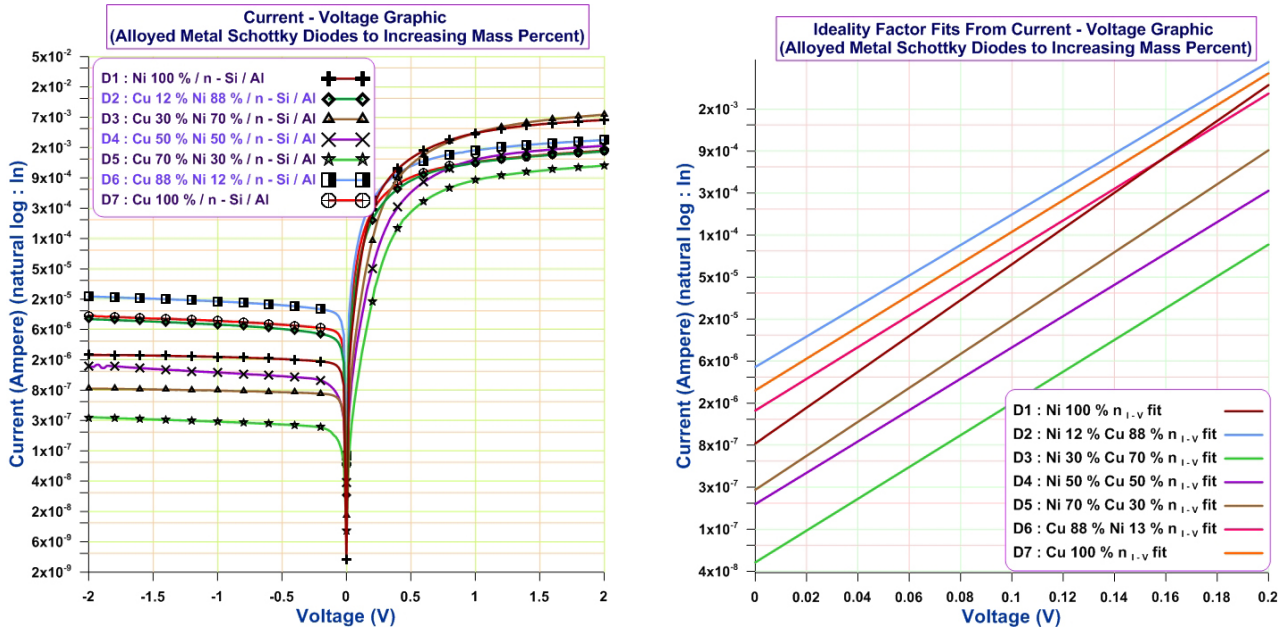

Figure 2. a. The forward and reverse bias current versus voltage (ln (I)–V) graphics for CN types. b. Ideality factor fits from current versus voltage (ln (I)–V) graphics.

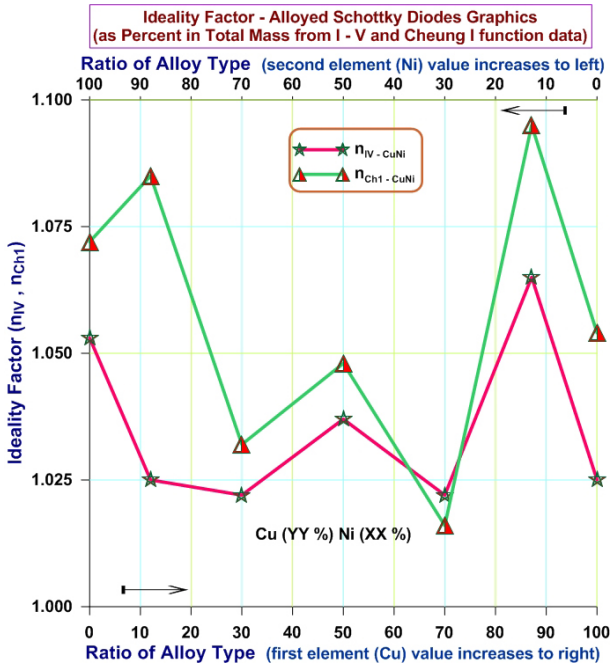

Figure 3. Ideality factor (from I–V) versus alloy type as a percent of alloyed metal/n–Si/Al Schottky diodes.

2.4. Barrier height (BH) and work function

BH is examined for the different metal types related to the alloy Schottky diode (see Table 1 in Ref. 10, Table 1 in Ref. 12, and Table 3 in Ref. 14). The BH is also used to determine the main features of the diode. It is obtained from the following formula [1,4,5]:

$$\Phi_{BH} = \frac{kT}{e} ln \left[\frac{AR^* T^2}{I_0} \right]. \tag{3a}$$

The values of BH are extracted from three data sets: $I-V$, C_s-V, and Ch2. Figure 4 shows the value of BH versus the alloy metal ratio. The green line, pink line, and brown line in Figure 4 represent the three different datasets, $I-V$, C_s-V, and Ch2, respectively. The behavior of the three lines is almost identical. They increase linearly to 70%.

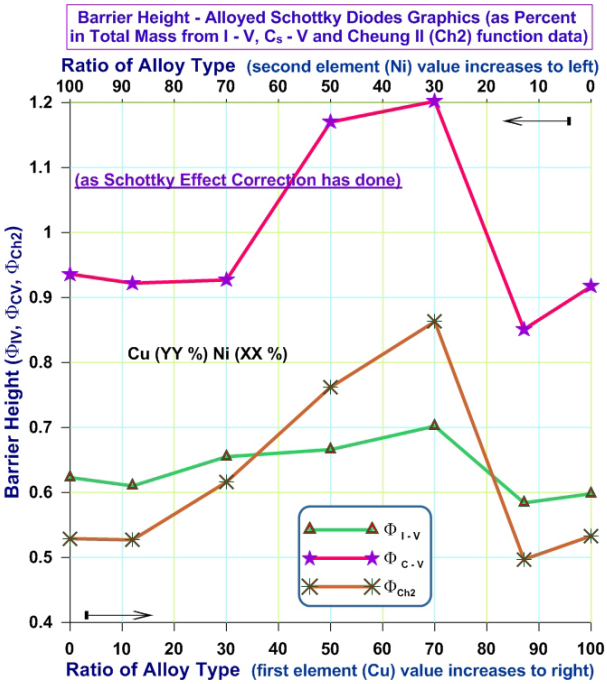

Figure 4. Barrier height (from I–V, C$_s$–V) versus alloy type mass percentage (Table 1).

Let us examine how the values of BH change with different ratios of the first metal (Figure 4). The values of BH$_{I-V}$ (green line) stayed almost constant at 10% and linearly increased to 70%, then decreased to 90% and then stayed almost constant. The values of BH$_{Cs-V}$ (pink line) stayed constant up to 30% and then linearly increased to 70%, decreased to 90%, and then increased again up to 100%. The values of BH$_{Ch2}$ (brown line) stayed almost constant at 10%, then increased to 70%, decreased abruptly to 90%, and then increased slowly to 100%. As seen from Figure 4, the values of BH vary with the varying mass percentage ratio of the first metal in the compound.

To understand Figure 4, we check the relationship between the work function and the barrier height. The work function is given as the value of semiconductor affinity plus the barrier height [4–7]:

$$W_m = \Phi_{BH} + \chi_S. \tag{3b}$$

Due to the varying value of the barrier height related to the mixing ratio of the metal alloy (with a constant value for semiconductor affinity), the work function value also varies. From Figure 4, it is clear that the work function value depends not only on the alloy metal ratio but also the type of metal (for example, Cu or Ni). We do not know any functional relationship between the element mass ratios of alloy compounds. Nevertheless, the correlation between the element mass ratio and the alloy compound could be either linear or exponential.

2.5. Cheung functions

Cheung functions are fundamental in the calculation of Schottky parameters. They are also used to check the results of Schottky parameters extracted from I–V or C–V plot fitting. For instance, the series resistance and barrier height are obtained from the Cheung functions given below [2,9,10] (Figure 5a). Figure 5b shows the changing of the ratio of alloy mass percent (m_p %) in serial resistance, too.

$$H(I)_{Ch1} = dV/d(\ln I) = IR_s + n_{IV}kT/e \quad ; \quad H(I)_{Ch2} = IR_s + n_{Ch1}\Phi_{BH}. \tag{4}$$

The Cheung I equation is symbolized for similarity as $H(I)_{Ch1}$.

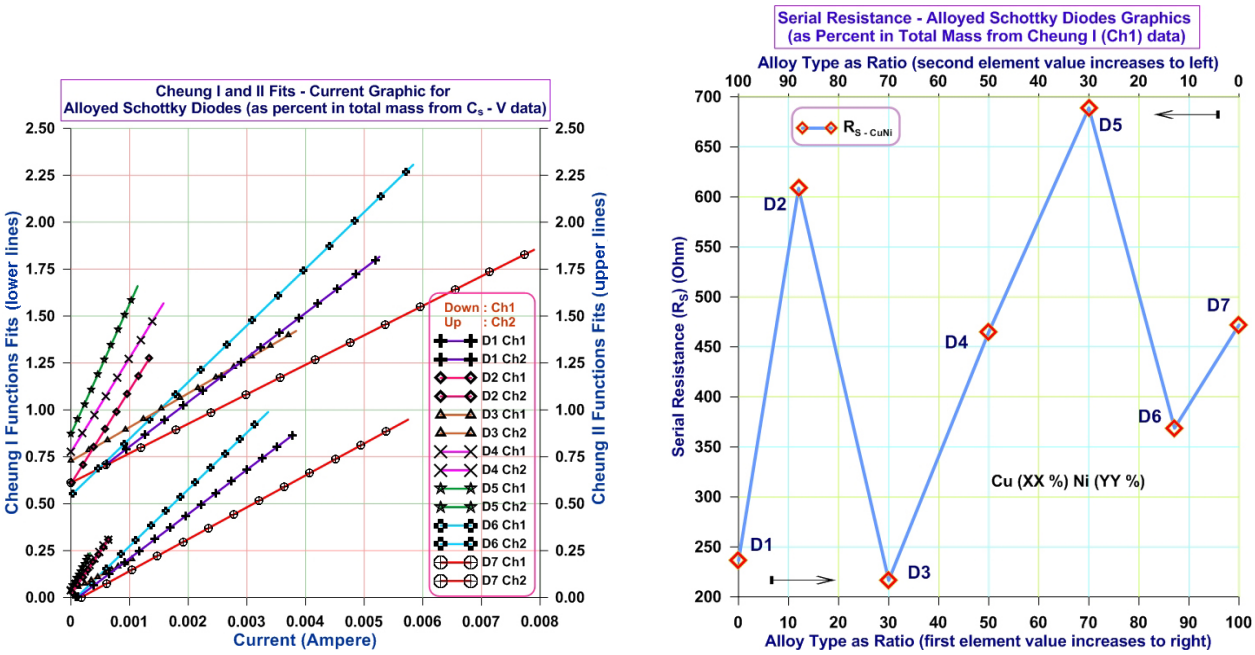

Figure 5. a. Fitting of Ch1 and Ch2 functions versus current. b. Serial resistance versus ratio of alloy type.

2.6. C_s –V graphics

C_s–V measurements of alloyed metal/n–Si diodes were carried out at a frequency of 250 kHz at room temperature in the dark. Figure 6 represents the fitting lines of alloyed metal/n–Si/Al. We drew a C_s^{-2} versus V graph (Figure 6) and fit it to obtain built-in potential values for the Schottky alloyed metal/n–Si/Al diodes. The slope of the fit informs us about donor concentrations for alloyed metal diodes. In addition, the built-in potential value is obtained from the point where the fitted slope intercepts the V-axis. After obtaining the built-in potential, donor concentration, ideality factor, and barrier height, we are ready to calculate the remaining parameters [1,9,11].

3. Depletion length

3.1. General depletion length

If pure metal is evaporated onto the semiconductor surface in a vacuum medium, thermal electrons move from the semiconductor to the metal, while holes move from the metal to the semiconductor due to the different work functions, and recombination progress occurs at this time. This process is known as a contacting process. The

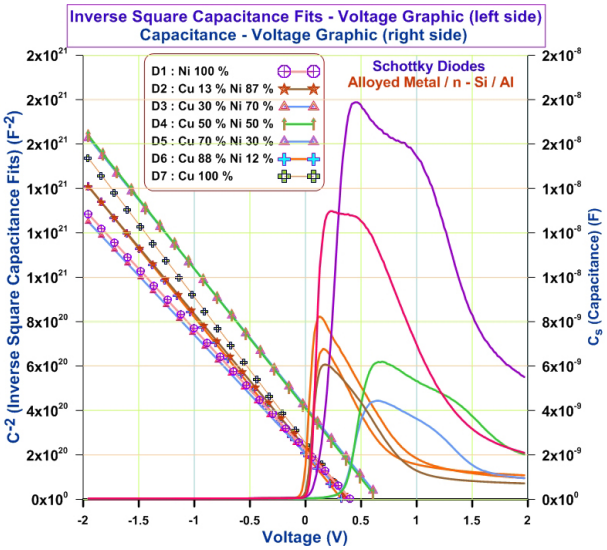

Figure 6. Fitting of inverse square capacitance–voltage (C^{-2}–V) versus voltage graphic and capacitance–voltage (C–V) graphic.

number of electrons in the metal–semiconductor junction will decrease due to the recombination progress and this results in a high-resistance zone where no charge carriers are located. When the semiconductor Fermi level and the metal Fermi level reach the same level, the contact formation process ends. This process is known as Fermi level pinning [1,3]. Therefore, positive charges occur between the metal and semiconductor side (namely, in the MS junction) and the uncharged region is built inside the semiconductor. In addition, we have a space charge zone in between the semiconductor and metal regions [3,4]. This zone is depleted of electrical charge. As we mentioned above, a potential field zone occurs due to interface polarization, which is the reason for having built-in potential [1,9]. Furthermore, built-in potential behaves like an interface layer. In addition, the difference between the semiconductor work function and the metal work function gives the built-in potential value, which acts as the BH when moving electrical charges. The built-in potential active zone is called the depletion region. Perpendicular to the diode surface, the size of the depletion region is called the depletion layer length or depletion length (DL). The DL is obtained from solving Poisson's equation for a voltage–distance equation, which is a quadratic function [1,3,9].

In the absence of applied voltage or the presence of built-in potential ($V_{bi} \neq 0$), the formula for L_{DL0} is given as follows [1,3,4,9]:

$$L_{DL0} = \sqrt{\frac{2\varepsilon_0 \varepsilon_S V_{bi}}{eN_D}} = \sqrt{\frac{2\varepsilon_0 \varepsilon_S (\varphi_M - \varphi_S)}{e^2 N_D}}, \tag{5}$$

where L_{DL0} is the zero bias depletion length, ε_s is the relative dielectric constant, ε_0 is the dielectric constant of space, V_{bi} is the built-in potential, e is the electron's charge unit, φ_M is the work function of the metal, and φ_S is the affinity of the semiconductor. In the presence of applied voltage and built-in potential, the formulae for forward and reverse bias conditions are written respectively as follows:

$$L_{FB} = \sqrt{\frac{2\varepsilon_0 \varepsilon_S (V_{bi} - V_a)}{eN_D}} \quad , \quad L_{RB} = \sqrt{\frac{2\varepsilon_0 \varepsilon_S (V_{bi} + V_a)}{eN_D}}, \tag{6}$$

where V_a is the applied voltage.

We used Eq. (6) in the case of L_{FB} and L_{RB} to obtain the corresponding depletion length values and plotted the depletion length versus the applied voltage. We applied 0 to 4 V for L_{FB} and –4 to 0 V for L_{RB}, as seen from Figure 7. As also seen from Figure 7, the depletion lengths versus voltage curves are equal but have mirrored symmetry in the case of L_{FB} and L_{RB}.

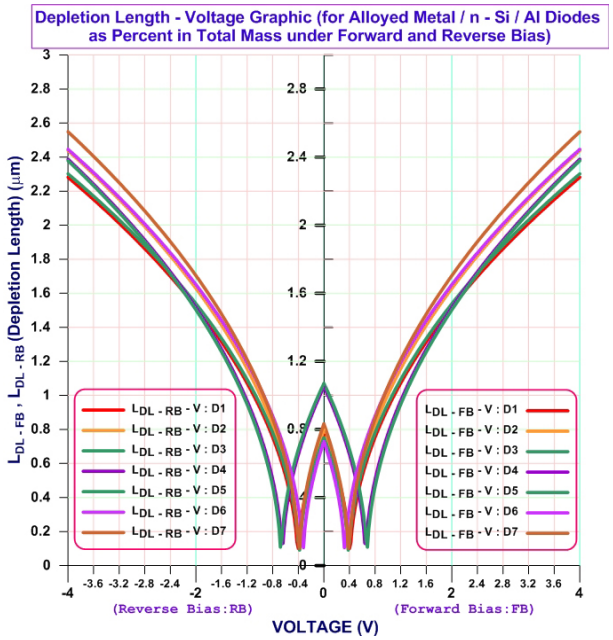

Figure 7. Depletion length versus voltage (L_{DL}–V) graphics.

3.2. Differential depletion length

How we can explain the decreasing depletion length in the case of forward bias, or the increasing depletion length for reserve bias? DDL was researched in the literature [9]. However, DDL is given either in equation form or graphical form. Therefore, we give two new formulae for DDL in the case of forward and reverse bias conditions, respectively:

$$\boldsymbol{\Delta L_{DL-FB} = L_{DL-FB} - L_{DL0} \Rightarrow L_{FB} = L_{DL0}\left[\sqrt{1 - \frac{V_a}{V_{bi}}} - 1\right]}, \tag{7}$$

$$\boldsymbol{\Delta L_{DL-RB} = L_{DL-RB} + L_{DL0} \Rightarrow L_{RB} = L_{DL0}\left[\sqrt{1 + \frac{V_a}{V_{bi}}} + 1\right]}. \tag{8}$$

According to the new formulae, we obtained values for DDL and then plotted DDL versus applied voltage ($\Delta L_{DL} - V$). Carefully analyzing Figure 8, it is seen that the characteristics of differential depletion length change with applied forward or reverse bias [4,9].

Regardless of applied voltage, DDL has a turning point on the V-axes at the built-in potential value (Figures 7 and 8). We also illustrate how the depletion layer changes with applied voltage (Figures 9a and 9b).

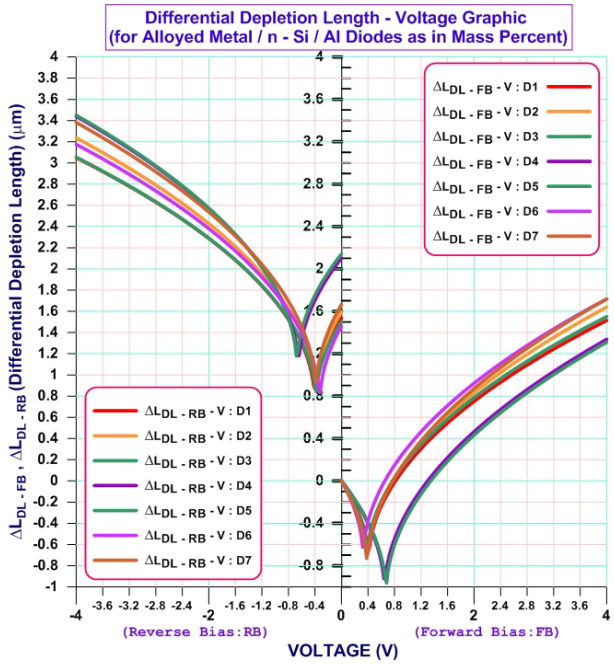

Figure 8. Differential depletion length versus voltage ($\Delta L_{DL} - V$) graphics.

3.3. Zero bias depletion length

The zero bias depletion length (ZDL) is described in a steady state. In other words, application potential (V_a) is zero while the built-in potential is not in the system ($V_a = 0$; $V_{bi} > 0$) [3,4,9]. The ZDL is the triangulation (or turning) point for DDL in the case of forward and reverse bias (see Figure 10).

In order to draw the zero bias depletion length versus increasing mass percentage of the first alloy element, we used Eq. (5) to plot Figure 10. It is seen from Figure 10 that the diode line decreased first to 30%, then increased to 70%, and then sharply decreased to 90% before increasing to 100%. The reason could be the effect of donor density rate and varying of the alloy ratio in the interface layer (Table 2). The depletion length depends on not only the donor concentration but also V_{bi} (built-in potential) in the MS Schottky diode (see Figure 9b). V_{bi} is equal to the difference between metal and semiconductor work functions (Φm–Φs; for n-type, rectifying contact), and the work function depends on the rate of element masses in the alloy.

3.4. Expansion of a series of differential depletion lengths (ExDDL)

If the square root part of the differential depletion length formula is expanded by a series, line equations for forward and reverse bias can be obtained, respectively, as follows [9]:

$$\boldsymbol{\Delta L_{ExDL-FB} = L_{DL-FB} - L_{DL0} \Rightarrow L_{ExDL-FB} = L_{DL0}\left(-\frac{V_a}{2V_{bi}}\right)}, \tag{9}$$

$$\boldsymbol{\Delta L_{ExDL-RB} = L_{DL-RB} + L_{DL0} \Rightarrow L_{ExDL-RB} = L_{DL0}\left(\frac{V_a}{2V_{bi}} + 2\right)}. \tag{10}$$

To analyze the graph (Figure 11a) obtained from Eqs. (9) and (10), it is seen that fits of the $ExDDL_{FB}$ obey a linear equation and their slopes have a negative value in the case of forward bias. However, fits of

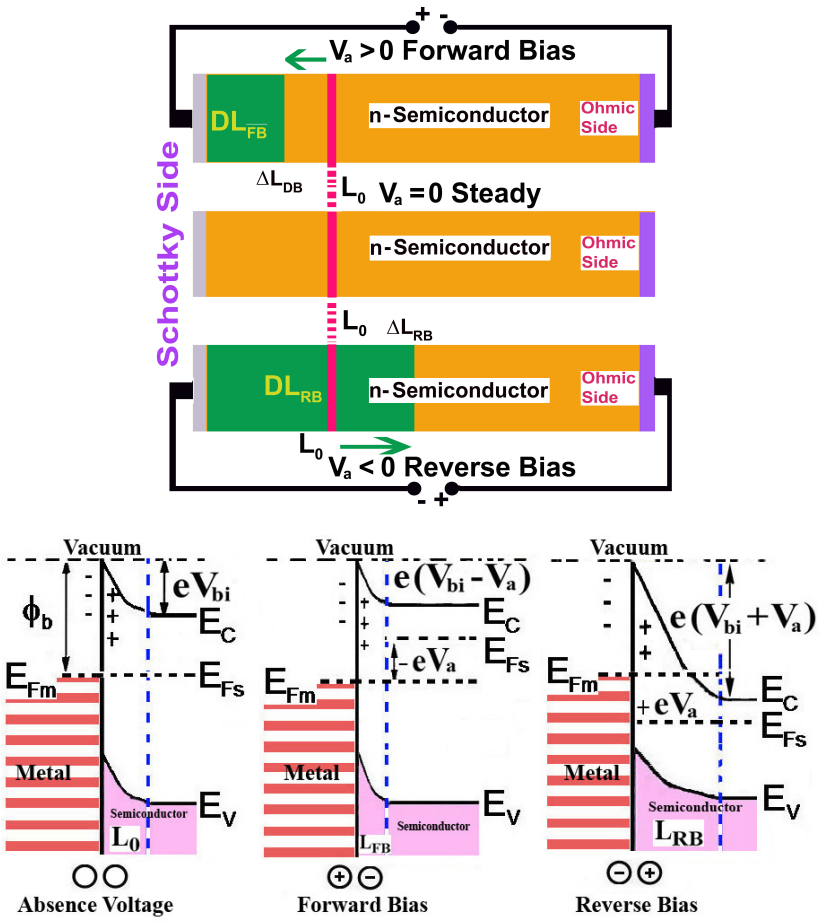

Figure 9. a. Illustration of differential depletion length for Schottky diodes. b. Band diagram of built-in potential in the absence of applied voltage and in the presence of applied voltage (forward and reverse bias) for Schottky diodes.

Table 2. Other parameter values for alloyed metal/n–Si/Al Schottky diodes (from I–V, C–V data).

Diode code	Built-in potential (eV)	Donor density (cm^{-3})	Depletion length (μm) ($V_a = 0$)	Interfacial thickness (D_{it})	Interfacial state density (eV^{-1} m^{-2})	Effective Fermi energy (eV)	Serial resistance (eVΩ)
D1	0.407	9.076 e14	0.768	1.087e–10	8.354 e15	0.550	236.329
D2	0.387	7.992 e14	0.798	1.934e–10	1.615 e15	0.544	608.654
D3	0.386	9.118 e14	0.746	9.673e–11	3.389 e15	0.550	216.658
D4	0.650	7.727 e14	1.052	3.202e–10	1.528 e15	0.543	464.823
D5	0.673	7.728 e14	1.070	1.392e–10	2.354 e15	0.543	688.926
D6	0.327	8.076 e14	0.729	1.161e–10	9.670 e15	0.545	368.868
D7	0.386	7.314 e14	0.833	1.495e–10	2.305 e15	0.541	471.977

the $ExDDL_{RB}$ also obey a linear equation, but their slopes have a positive value in the case of reverse bias. Expansion of a series of differential depletion length equation fits obeys the $m_1 - m_2 \approx 0$ rule in analytical geometry. To be more specific, we also draw data belonging to D6 (Figure 11b). As seen from Figure 11b, we

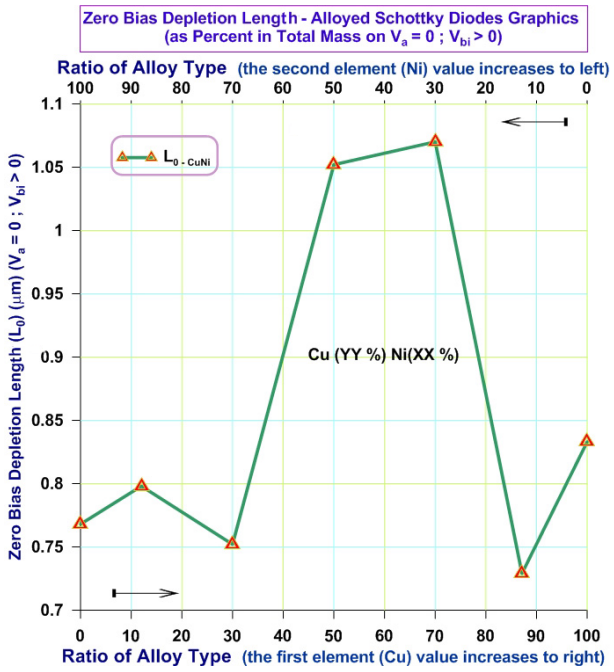

Figure 10. Zero bias depletion length versus the ratio of alloy mass percent ($L_{DL0} - m_p$ %) ($V_a = 0$ or $V_{bi} > 0$).

have an intersection point of the $ExDDL_{FB}$ and $ExDDL_{RB}$ lines. If we project this intersection point onto the x-axis, this point equals two times the built-in potential ($2 \times V_{bi}$).

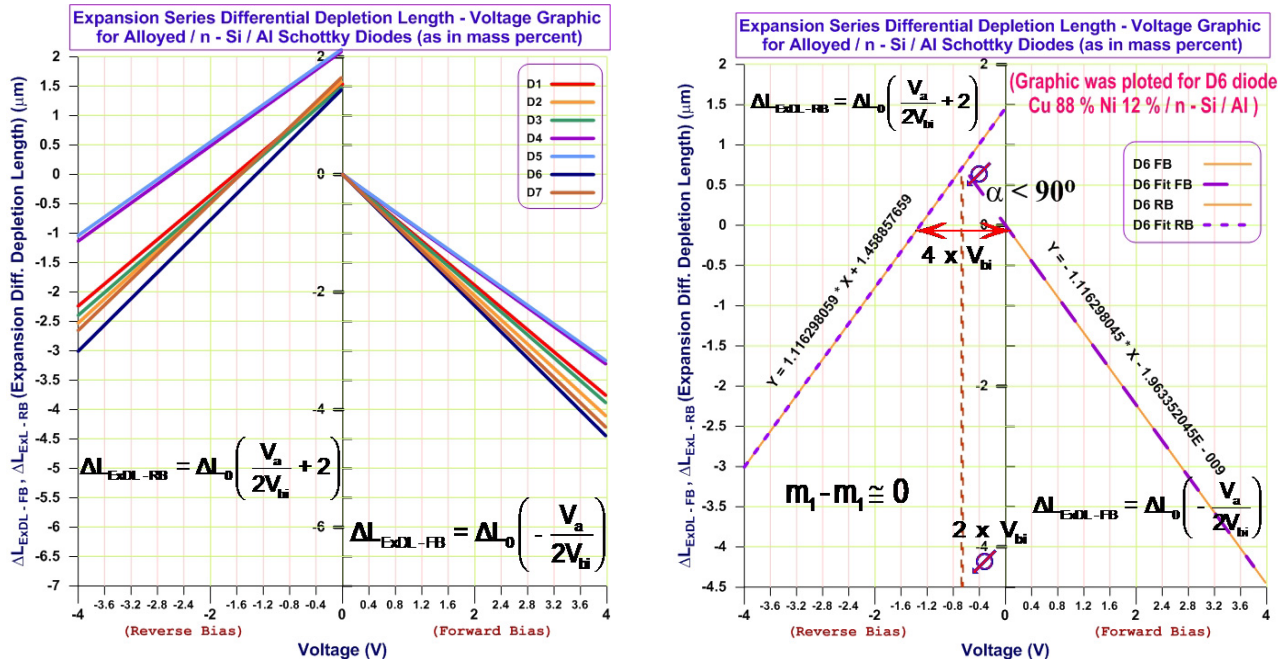

Figure 11. a. Expansion of a series of differential depletion length–voltage ($\Delta L_{ExDL} - V$) graphics for Schottky diodes. b. Expansion of a series of differential depletion length fits–voltage ($\Delta L_{ExDL} - V$) graphics for Schottky diodes (data for D6 diode have been chosen randomly).

4. Conclusion

The fits of DDL expanded in a series follow the $m_1 - m_2 \approx 0$ rule. In Figures 11a and 11b, the slopes are almost equal to each other with very little error. Moreover, in the line equation y = ax ± b, a slightly different ± b may be obtained. In our case, the y= ax ± b equation could be approximated to y ≈ ax ± b. This situation may be characteristic of the diode. The calculations of DDL, ExDDL, and DL are essential parameters to obtain the built-in potential of the diode. As seen from Figures 7, 8, 11a, and 11b, the curves show a turning point at the built-in potential and have a vital role for Schottky diode parameters. It was seen that all Schottky diode characteristics were changed by increasing the alloy mass percentage. For instance, Schottky parameters show some fluctuations with increasing rates of mass percentage of copper in the alloy (see Figures 3 and 4). We also stress that the results obtained from forward and reverse bias are correlated to each other at direct current, whereas forward bias is independent of reverse bias. In this study, we found an equation for the ExDDL obeying the $m_1 - m_2 \neq -1$ rule (it obeys the $m_1 - m_2 \approx 0$ rule). It is noted that the differential depletion capacitance (ExDDC) equation was found and it obeys the $m_1 - m_2 = 0$ rule (referring to the parallel lines) [9]. In this article, we tried to give some insight into the essential Schottky diode features, especially L_0, DL, DDL, and ExDDL (see Figures 7–11).

Acknowledgments

The author thanks Assistant Professor Murat Aycibin for technical and linguistic suggestions. This work was supported by the Research Fund of Yüzüncü Yıl University. The project number was 2014-FBE-D008.

References

[1] Korkut, A. PhD, Van Yüzüncü Yıl University, Van, Turkey, 2015.

[2] Cheung, S. K.; Cheung, N. W. *Appl. Phys. Lett.* **1986**, *49*, 85-87.

[3] Sharma, B. L. *Metal-Semiconductor Schottky Barrier Junctions and Their Applications*; Plenum Press: London, UK, 1984.

[4] Schroder, D. K. *Semiconductor Material and Device Characterization*, 3rd ed.; J. Wiley & Sons: New York, NY, USA, 2006.

[5] Sze, S. M. *Physics of Semiconductor Devices*, 2nd ed.; J. Wiley & Sons: Singapore, 1981.

[6] Ng, K. K. *Complete Guide to Semiconductor Devices*; McGraw-Hill Inc.: New York, NY, USA, 1995.

[7] Card, H. C.; Rhoderick, E. H. S. *J. Phys. D.* **1971**, *4*, 1589-1601.

[8] Horvath, Z. J. *J. Appl. Phys.* **1988**, *63*, 976-978.

[9] Korkut, A. *Sur. Rev. Lett.* **2018**, *25*, 1850043.

[10] Reddy, Y. M.; Nagaraj, M. K.; Naik, S. S.; Reddy, V. R. *J. Mod. Phys.* **2012**, *3*, 538-545.

[11] Hudait, M. K.; Kurupanidhi, S. B. *Mat. Sci Eng.* **2001**, *B87*, 141-147.

[12] Mehari, S; Gavrilov, S. A.; Cohen, S.; Shekhter, P.; Eizenberg, M.; Ritter, D. *Appl. Phys. Lett.* **2012**, *101*, 072103.

[13] Wong, P. K.; Kwok, C. T.; Man, H. C.; Cheng, F. T. *Corr. Sci.* **2012**, *57*, 228-240.

[14] Huang, T.; Jean, S. M. *J. Appl. Phys.* **1994**, *75*, 7519-7525.